SRF CAVITY BREAKDOWN CALCULATION PROCEDURE USING FEA-SOFTWARE

Roman Kostin#, Alexei Kanareykin, Euclid Techlabs, LLC, Solon, Ohio, USA
Ivan Gonin, Fermilab, Batavia, IL 60510, USA
Evgeniy Zaplatin, Forschungszentrum Juelich, Juelich, Germany

Abstract

SRF cavity thermal breakdown can be analyzed analytically using thermodynamics equation. This technique is suitable for simple geometries when surface magnetic field variation can be omitted. Thermal radiation effect which is crucial for SRF gun calculations is also hard to implement properly because of complicated geometry. All of these can be overcome by using multiphysics FEA-software. This paper shows the procedure of cavity thermal breakdown calculation in coupled multiphysics analysis with dependable parameters.

INTRODUCTION

The goal of this work was implementation of thermal multiphysics analysis of SRF cavities in FEA software with temperature dependant parameters such as surface resistance and thermal conductivity. Kapitza resistance was assumed to be constant with constant bath temperature. ANSYS APDL scripts were developed to perform the analysis.

3.9 GHz elliptical cavity QvsB curves which were obtained at Fermilab for DESY FLASH module were used to check ANSYS results. Thermal conduction coefficient, Kapitza conductance and surface resistance was obtained for better matching with measured QvsB curves. The first attempts to fit the curves were done in the reference [1]. Simple model with constant thermal conduction coefficient was implemented in Mathcad. The results did not show an agreement for each case. In this paper 9 cell 3.9 GHz elliptical cavity data was used to fit ANSYS results and show a good agreement for almost the same quench fields. This proves the accuracy of developed ANSYS macros and opens the way to use it for different geometries as a “plug and play” solution.

The developed algorithm also was tested on 1.4 cell HZB SRF gun [2]. It represents L-band 1.4-cell SRF gun with warm cathode which has a very tiny gap between the cathode and niobium walls in superconducting state. Although, global thermal breakdown is not possible in L-band cavities, superheating field is greater than critical magnetic field of niobium, accurate thermal analysis is required to determine cathode temperature and its longitudinal thermal expansion. The thermal radiation was not included in our simulations yet but will be implemented in later works.

r.kostin@euclidtechlabs.com

3.9 GHz CAVITY MULTIPHYSICS ANALYSIS

Global thermal breakdown of SRF cavities is determined by temperature dependence of surface resistance which in terms depends on RF magnetic field heating. Heat flux from RF heating depends on the temperature:

$$q = \frac{R_s}{2} \cdot H_\tau^{\ 2} \quad (1),$$

$$R_s = R_{BCS}(T) + R_{Res} \quad (2),$$

where q - thermal heat flux, R_{BCS} - temperature dependant BCS surface resistance, R_{Res} - residual constant surface resistance and H_τ – surface magnetic field.

Heat flux from RF heating changes temperature distribution which in its term should change the applied heat flux at constant fields. Special APDL macro was developed to take into account this heat flux dependence on temperature by iterative thermal calculations. Surface resistance, thermal conductivity and Kapitza resistance has been set as functions of temperature, i.e. their values are calculated by ANSYS according to temperature distribution. Kapitza resistance depends on bath temperature which is constant but could be evaluated for different regimes which eliminate the need of correction for different bath temperatures. There are only two input parameters - magnetic field and bath temperature, the others were set through functions.

Fermilab 3.9 GHz 9 cell cavity experimental data (QvsB curves) were used to compare with simulation results. The corresponding thermal conductivity, Kapitza and surface resistance were required to match experimental curves with simulation results. A 1D simplified model was developed to find proper material properties and save time on simulation. The length of the model equals to the cavity wall thickness. Heat flux was applied to one side and convection coefficient that equals to Kapitza conductance for the other side. Temperature dependent thermal conductivity was also applied. Several Kapitza resistance models (Amrit1, Amrit3, Mittag), residual resistance and thermal conductivity coefficients (see Fig. 1) were used to obtain global thermal breakdown at fields as close as possible to quench fields from the experimental data. The calculated results can be found in Table 1.

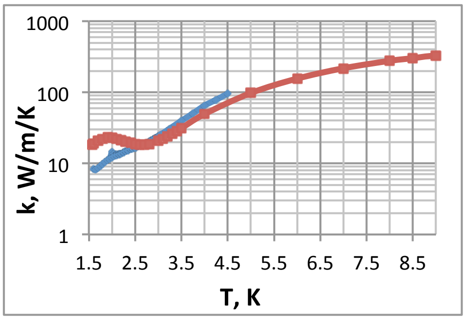

Figure 1: Thermal conductivity coefficients of Nb RRR300 for different crystal structures from Wah Chang measured at Fermilab [3]: red curve - large grain, blue curve – fine grain.

Table 1: 1D Model Simulation Result Data

Thermal Conductivity	Large Grain			Fine Grain		
Wall thickness, mm	2.8	2.6	2.6	2.8	2.6	2.6
h_{kap}, Amrit3	*	*		*	*	
h_{kap}, Mitag			*			*
B_{quench}, mT	120	122	103	108	110	96

It was detected (Table 1) that quench field does not have a strong dependence on wall thickness. The same is true for residual resistance which was about 10 nOhm for these simulations. But the quench field strongly depends on thermal conductivity, BCS resistance and Kapitza conductance which is 9500 [W/m^2/K] for Amrit3 [4] and 5000 [W/m^2/K] for Mittag [5] at T_{bath}=2 K. A thermal conductivity data is shown on Figure 1. The 3.9 GHz cavities were built from fine grain Niobium, with 2.6 mm cavity wall thickness, annealed and BCPed and had a quench around 120 mT. According to cavity history, the suitable Kapitza model is Amrit3 but 1D model shows a good agreement for large grain material in this case. It is important to emphasise that this model does not include magnetic field variation along the cavity which was found to be important in 2D and 3D simulations. The typical thermal breakdown temperature rise can be seen on Fig. 2.

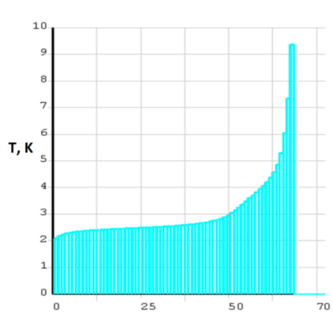

Figure 2: 1D model temperature rise during quench.

The next step was implementation of magnetic field distribution along the cavity. A classical ANSYS version was used to find electro-magnetic field distribution in the cavity. 3D ANSYS model was used for RF field simulations. A special macro was developed to make a thermal breakdown analysis in 3D but taking into account axial symmetry of the cavity the macro was upgraded to 2D thermal calculations with 3D RF part. It still does calculate the Q factor even in 2D case. Different cases were compared such as 90/30 degree 3D/2D model of 9/single cell cavity (see Fig. 3 for 90 degree 9 cell 3D model simulation). It was found that the difference of simulation results in terms of quench field is within few mT. These results allow using 2D thermal model with 3D RF part to save the simulation time. The simulated QvsB curves are shown on Fig. 4.

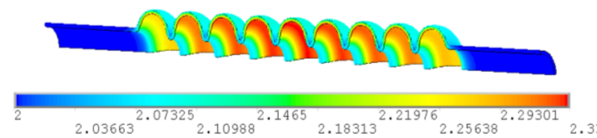

Figure 3: 3.9 GHz 9 cell cavity temperature distribution just before the quench (Fine grain, Amrit3, Rres=10nOhm).

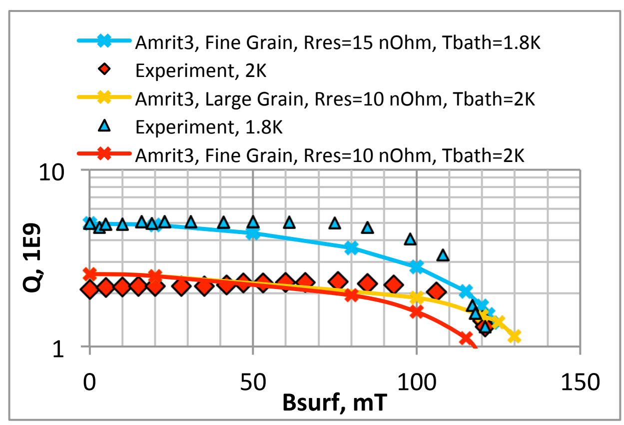

Figure 4: 3.9 GHz 9 cell QvsB curves.

As it was mentioned before, the residual resistance does not have a significant influence on quench field. Typical numbers of residual resistance are around 10 nOhm while the BCS resistance is several hundred nOhms at 3.9 GHz and T=2.3 K, which is the temperature just before the quench (see Fig. 3). That also can be seen from Figure 4 where Rres=10 nOhm for 2 K case and Rres=15 nOhm for 1.8 K. The quench fields for different bath temperatures and corresponding thermal conductivity are almost the same. 2D results show that magnetic field variation implementation increased the quench field for large grain and fine grain cases by 10 mT. The large grain case, which showed a good agreement in 1D simulation model has 130 mT quench field in 2D. Fine grain has around 120 mT quench field in 2D simulation which is close to experimental data

The simulated curves have a mid-field slope while the experimental data does not. The same discrepancy was

ISBN 978-3-95450-178-6

found in previous work [1]. Material properties were taken according to the cavity processing history. Quench field was obtained close to experimental that proves the applied algorithm.

1.4 CELL HZB SRF GUN MULTIPHYSICS ANALYSIS

The developed algorithm was used for 1.4 cell HZB gun [2] multiphysics simulations. It represents an L-band 1.4-cell SRF gun with warm cathode which has a very tiny gap between the cathode and niobium walls in superconducting state. A 10 W laser shines on the cathode for electrons extraction.

A known problem of that gun is RF field leakage to the cathode normal conducting part (see Fig. 5). An additional choke filter might be implemented to prevent that. Surface resistance for all parts was set as niobium in our simulations. Corresponding temperature distribution is shown on Figs. 6 and 7. Thermal conductivity of Nb RRR 300 was used for niobium parts and conductivity of high RRR copper was used for everything else. A surface magnetic field (Bpk=100 mT) heating caused only several hundredths degrees of temperature rise. Maximal temperature is on the cathode tip and equal to 93 K. This temperature distribution gives a 160 micron elongation of the cathode assembly (see Fig. 8).

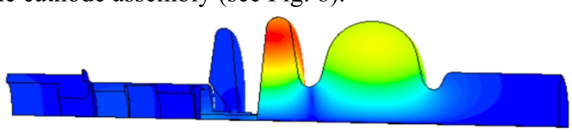

Figure 5: Magnetic field distribution.

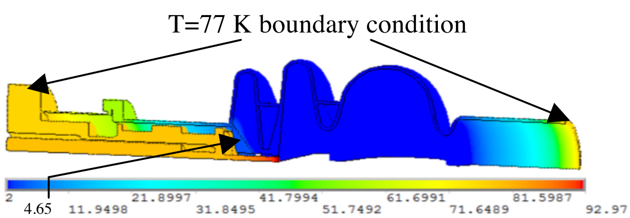

Figure 6: Temperature distribution, K.

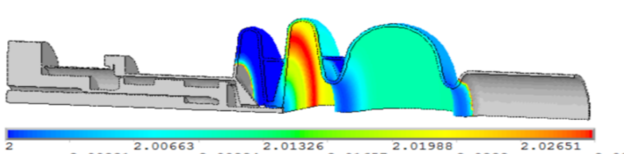

Figure 7: Temperature distribution, K.

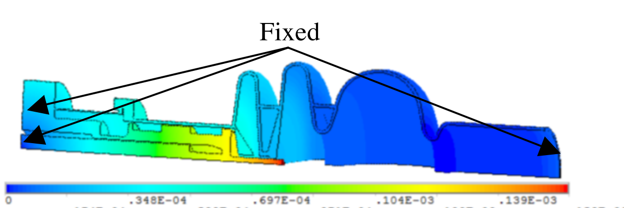

Figure 8: Temperature deformations, m.

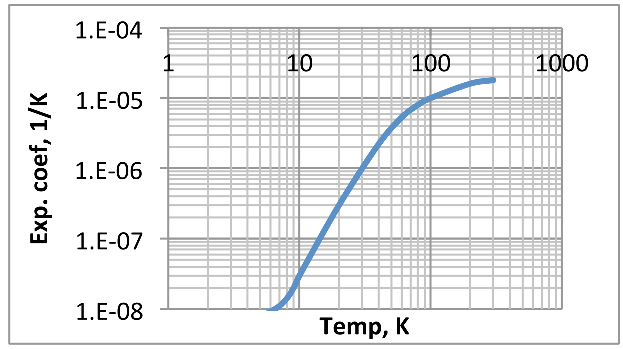

Figure 9: Copper thermal expansion coefficient.

A copper thermal expansion coefficient $\alpha_{Cu}(T)$ has been set as a function of temperature in ANSYS and is shown on Fig. 9. The simple 1D calculation of cathode tip elongation with a uniform 80 K temperature rise for all cathode part, expansion coefficient at 80 K (α_{Cu} = 8E-6 1/K) and for cathode stack length (0.23 m) results in 160 μm cathode tip elongation. This is the same result of numerical simulations which detects that expansion coefficient temperature dependence was not included by ANSYS and only a single value was taken at a certain temperature point. A similar 1D calculation with integrated expansion coefficient at 80 K (α_{int}=integral($\alpha_{Cu}(T)$* dT)=1.56E-4) results in a 40 μm elongation instead of 160 μm.

CONCLUSION

Special APDL macro was developed to take into account heat flux dependence on temperature by iterative thermal calculations. Wall thickness and residual resistance do not affect much on quench field. Thermal conductivity, Kapitza conductance and residual resistance were chosen according to FNAL 3.9 GHz elliptical cavity processing history. The simulations showed a good agreement with experimental data which proves the applied algorithm.

The developed macro was used for 1.4 cell HZB gun calculations. Magnetic field heating caused very small temperature rise on the cavity cell walls – around 0.03 K, which was expected as soon as global thermal breakdown is not an issue for L-band cavities. RF field leakage was detected in the cathode part with the temperature rise at back wall of the choke-cell. Simulated model showed a 160 μm thermal expansion of the cathode instead of 40 μm by 1D calculation. That detects that expansion coefficient value in ANSYS was taken at certain point and was not integrated.

ACKNOWLEDGMENT

We would like to thank Nikolay Solyak, Mohamed Hassan and Sam Posen from Fermilab Technical Division for fruitful discussions and considerations.

REFERENCES

[1] N. Solyak, et al., WEP41, in Proc. of SRF2007, Albuquerque, NM, USA, http://www.jacow.org/

[2] A. Burrill, et al., "Processing and Testing of the SRF Photoinjector Cavity for BERLinPro", WEPRI005 Proceedings of IPAC2014, Dresden, Germany, http://jacow.org/

[3] S. Koshelev, Research of thermal properties of superconducting niobium for SRF cavities. Moscow, 2013.

[4] J. Amrit, et al. "On intrinsic thermal limitations of superconducting cavities: Kapitza resistance." Advances in Cryogenic Engineering: Proceedings of the Cryogenic Engineering Conference-CEC. Vol. **613**(1), AIP Publishing, 2002.

[5] K. Mittag, "Kapitza conductance and thermal conductivity of copper niobium and aluminium in the range from 1.3 to 2.1 K." Cryogenics **13**(2), 94 (1973).

ISBN 978-3-95450-178-6